Thin Film Structure of Triisopropylsilylethynyl-Functionalized Pentacene and Tetraceno[2,3-b]thiophene from Grazing Incidence X-Ray Diffraction

Stefan C. B. Mannsfeld, Ming Lee Tang, and Zhenan Bao*

Over the past couple of years, triisopropylsilylethynyl (TIPS)-functionalized acenes[1] have been gaining importance as a new type of highly soluble, air-stable, high-performance p-type organic semiconductor for organic electronics applications such as organic field effect transistors (OFET), inverters, printed circuitry, etc.[2,3] A more recently synthesized derivative, TIPS-tetraceno[2,3-b]thiophene,[4] outperforms TIPS-pentacene[5] in vacuum-deposited thin films by about a factor of three (field effect mobility of 1.25 versus 0.4 cm^2/Vs). The electrical performance of poly-crystalline thin films of a given organic material depends on a variety of factors: the exact packing of the molecules in the grains, the density and type of boundaries between crystalline grains, and the chemical nature and purity of the interface between the substrate surface and the film.[6–12] With small aromatic molecules, the exact molecular structure and the packing of the aromatic cores are widely accepted to be the most crucial factor for the hole or electron conductivity within the crystalline grains (i.e., the material's intrinsic field effect mobility).[13–17] Common acenes, such as tetracene or pentacene, adapt a herringbone packing motif in both single crystal and thin film.[18] The packing of acene derivatives can be changed with peripheral substitutions on opposite sides of the short molecular axis. For example, 5.11-dichlorotetracene was found to have a face-to-face packing and a single crystal field effect mobility of 1.6 cm^2/Vs.[19] In the case of the TIPS-functionalized acenes, the bulkiness of the TIPS group forces the aromatic pentacene sub-units into a brick wall-like face-to-face arrangement.[18] This molecular arrangement was reasoned to be the major factor in the high performance of TIPS-pentacene thin film devices. However, detailed information on the molecular packing is available only for bulk single crystals, and the molecular packing of TIPS-functionalized acenes in thin films has not been directly determined to date. In fact, the discussion concerning the thin film transistor properties hinges entirely on the assumption that the thin film structures are identical to the respective single crystal structures, often inferred from similarities in the respective unit cell dimensions. It is well known that the molecular packing in thin films may be significantly different than that in the bulk structure, especially near the interface to the substrate. Examples for this are tetracene[20] and especially pentacene where, despite similar unit cell geometries in thin films and the bulk crystal, the molecular packing motifs in thin film phase and bulk phase are quite different and even depend on the film thickness.[15,21–23] The origin of this phenomenon is the chemical interaction between the molecules and the specific substrate surface the thin film is grown on. The charge transfer rate between the molecules is highly dependent on the exact alignment of the molecules. Therefore, the assumption that thin films grow in the same molecular packing motif as the bulk crystal packing is not always justified. Here, we utilized grazing incidence X-ray diffraction (GIXD) and crystallographic refinement calculations to determine the molecular packing of TIPS- tetraceno[2,3-b]thiophene (hereafter referred to as TIPS-thiotetracene) and TIPS-pentacene (**Figure 1**) in thin films on silicon oxide.

Previously, we applied this combination of methods to determine the molecular packing in pentacene,[15] tetraceno[2,3-b] thiophene,[20] and fluorene-bithiophene-fluorene.[24] A similar type of calculation was more recently reported for a perylene derivative.[25]

The geometry of the GIXD experiment is depicted in **Figure 2**a. The highly collimated synchrotron X-ray beam (monochromatic at $E = 12.73$keV), $\mathbf{k}_0$, strikes the surface under a grazing incidence angle α and the diffracted intensity (wave vector $\mathbf{k}$) is recorded on a 2D image plate detector (distance L). The incidence angle is kept fixed at 0.1°, which is below the critical angle of external reflection of the substrate (SiO_2), so

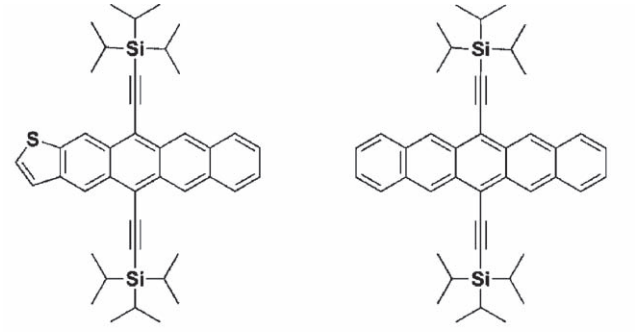

Figure 1. Chemical structure of TIPS-thiotetracene and TIPS-pentacene.

Dr. S. C. B. Mannsfeld
Stanford Synchrotron Radiation Lightsource
Menlo Park, CA, U.S.A
E-mail: mannsfel@slac.stanford.edu
M. L. Tang, Prof. Z. Bao
Department of Chemical Engineering
Stanford University, CA, U.S.A.

DOI: 10.1002/adma.201003135

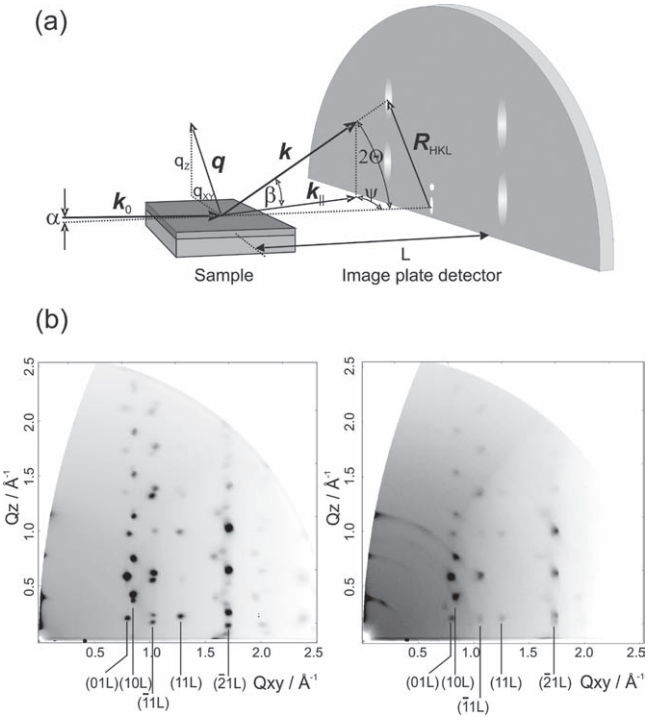

Figure 2. (a) Geometry of the GIXD setup. The incident beam $\mathbf{k}_0$ forms an angle α with the sample surface; the intensity of the scattered beam $\mathbf{k}$ is recorded by an image plate detector at a distance L. The in-plane component of the momentum transfer vector $\mathbf{q}$ is q_{xy}; the vertical component q_z. (b) GIXD images of 40 nm TIPS-thiotetracene (left) and TIPS-pentacene (right) on SiO_2. Indices are provided for the most intense Bragg rods.

that most of the beam intensity is focused into a surface-near region of the sample. Organic molecules are typically weak X-ray scatterers and thus often produce sufficient diffraction intensity only in synchrotron-based GIXD experiments. The diffraction patterns recorded on the image plate for the 40 nm thick films of TIPS-thiotetracene (left) and TIPS-pentacene (right) on SiO_2 are shown in Figure 2b.

The vacuum-deposited thin films of both molecules are 2D powders in which the a-b unit cell vectors of all grains are in the substrate plane but the azimuthal orientation is random. In the GIXD images this manifests in the diffraction peaks grouping on vertical Bragg rods, i.e. in a clear partitioning of the total photon momentum transfer $\mathbf{q}$ into in-plane (q_{xy}) and out-of-plane momentum transfer (q_z) for all peaks. The more intense Bragg rods are labeled with their respective Miller indices in Figure 2b. There is some arching visible in the TIPS-pentacene GIXD images. Unlike Laue diffraction where similar features form as result of a typically broad spectrum of X-ray wavelengths, in the present case of monochromatic incident X-rays these arcs mean that the TIPS-pentacene grains form a less than ideal 2D powder and exhibit some misorientation with respect to the substrate surface. In single crystals of TIPS-pentacene, destructive structural changes such as cracking were observed as side-effect of a phase transition occurring at about 120 °C.[26] While there is no indication for the presence of the high-temperature phase in the thin films, thermal disorder and cracking could in a similar fashion be a factor in the grain misorientation. The resulting higher-angle grain boundaries would readily explain why the electrical performance of the vacuum-deposited TIPS-pentacene in OFET devices is lower than in TIPS-thiotetracene devices.[4]

Before the peak positions were measured in the GIXD images, an image correction needed to be applied (see shape of diffraction images in Figure 2b) because the flat image plate records a distorted projection of the momentum transfer space (reciprocal space) of the sample surface. From the measurement of the diffraction peak positions in the distortion-corrected images, the unit cell parameters were extracted using a least-square-error fitting procedure (**Table 1**). While the unit cells are overall quite similar to their single crystal counterparts, the unit cells of both compounds are slightly more obtuse with one in-plane lattice vector (denoted b in here) being slightly elongated in thin films on SiO_2.

While the peak positions contain information on the periodicity in the crystalline grains, the peak intensities are used to extract information on the molecular alignment inside the unit cell. Since an area detector captures the whole spatial extent of the diffraction peaks, the integrated peak intensity is proportional to the maximum intensity I_{hkl}^{max}, as given by Equation 1:

$$I_{hkl}^{max} = I_0 \frac{e^4}{m_e^2 c^4} NPLDCT^2(q_z)\,|F_{hkl}|^2\,, \qquad F_{hkl} = \sum_j f_j(\mathrm{q}) e^{i\mathrm{q}r_j} \tag{1}$$

In Equation 1, I_0 is the incident beam intensity and N the number of unit cells in the film that satisfy the Bragg condition. Several correction terms ($PLDC$) have to be applied to the structure factor square $|F_{hkl}|^2$ to obtain the theoretically expected diffraction intensity. The factor P denotes the correction for the beam polarization (95% in-plane polarized at SSRL BL11–3); L denotes the Lorentz correction factor $1/\cos(\alpha)\sin(\psi)\cos(\beta)$. Although our GIXD setup involves no rotation of either detector or sample, a Lorentz correction is necessary because the film forms a 2D-powder in the substrate surface plane. For simplicity, an isotropic molecular mean square displacement $\langle U^2 \rangle$

Table 1. Lattice constants of the TIPS-thiotetracene and TIPS-pentacene thin films on SiO_2 in comparison to the respective single crystal data.

	a (Å)	b (Å)	c (Å)	α (°)	β (°)	γ (°)
TIPS-thiotetr.	7.61 ± 0.04	8.11 ± 0.04	16.66 ± 0.04	103.8 ± 0.5	89.0 ± 0.5	102.4 ± 0.5
TIPS-thiotetr. s.c.	7.63	7.66	16.67	102.1	89.6	98.6
TIPS-pentacene	7.70 ± 0.04	7.83 ± 0.04	16.78 ± 0.04	103.5 ± 0.5	88.0 ± 0.5	99.0 ± 0.5
TIPS-pent. s.c.	7.75	7.56	17.01	104.2	88.0	96.4

is assumed in the Debye Waller factor $D = \exp(-\langle U^2\rangle \mathbf{q}^2)$ that corrects for molecular vibrations. The term $C = \cos^3(2\Theta)$ corrects the peak intensities that were measured in the distortion-corrected **q**-space images as shown in Figure 2b rather than as-recorded images. The Fresnel transmitted wave intensity function $T^2(q_z)$ is different from 1 only for very small magnitudes of the out-of-plane momentum transfer q_z. It is worth pointing out that even though diffracted X-ray beams impinging the detector at different angles have traveled different distances in air, the attenuation by air scattering losses is very small at the photon energy of 12.73 keV and this effect is therefore neglected in Equation 1. In the expression for the structure Factor F_{hkl}, f_j denotes the complex and angle-dependent atomic scattering factors $f_i(q) = f_0(q) + f_1 + if_2$ of the jth atom in the unit cell. They were calculated using a Cromer-Mann function and corresponding coefficients.[27] The coefficients for the hydrogen factor were obtained by fitting literature data[28] to a Cromer-Mann function. The energy-dependent real and complex corrections to the scattering factors, f_1 and f_2, were obtained from Henke et al.[29]

With Equation 1 providing an expression for the theoretically expected peak intensity, a determination of the molecular alignment in the unit cell can be attempted using a crystallographic refinement algorithm. With the number of measurable peaks typically being on the order of 20 in the organic thin film GIXD images, a refinement of individual atom positions is not possible as the number of atoms in the molecules exceeds the number of data points available for fitting. However, the assumption that the molecules are rigid (i.e. the distances between all atoms on the molecule are retained) drastically reduces the number of fitting parameters from the number of atoms to the much more manageable three Euler angles per molecule in the unit cell. From the unit cell volumes of both materials it can be inferred that there is only one molecule in the unit cell. Thus, three molecular angles sufficiently describe the entire unit cell content. The assumption of rigid molecules is largely justified, especially for the aromatic pentacene and thiotetracene cores,[30,31] whereas it is less fitting for the TIPS side-groups. The molecular structures of both TIPS-pentacene and TIPS-thiotetracene were taken from the single crystals data.[4,5] In the case of TIPS-thiotetracene, significant defects in the single crystal molecular structure made it necessary to reconstruct the parts of the isolated molecule using the Parametric Model number 3 (PM3) semi-empirical method.

$$R = \sum_{q \in peaks} W_q \left(\left| F_{obs}(\mathbf{q}) \right| - k \left| F_{calc}(\mathbf{q}) \right| \right)^2,$$

$$k = \frac{\sum_{q \in peaks} W_q \left| F_{obs}(\mathbf{q}) \right| \left| F_{calc}(\mathbf{q}) \right|}{\sum_{q \in peaks} W_q \left| F_{calc}(\mathbf{q}) \right|^2} \quad (2)$$

The angular alignments of the TIPS-thiotetracene and TIPS-pentacene molecules in the thin film unit cell (Table 1) were determined by minimizing the crystallographic residual[32] [R in Equation (2)] which is a type of least square error between theoretical and experimental intensity values. The numerical minimization was achieved using the Monte Carlo method called Simulated Annealing (SA).[33] During the SA procedure, the molecular orientation is varied until the crystallographic residual becomes minimal. Integrated intensity values were measured for 30 (TIPS-thiotetracene) and 19 (TIPS-pentacene) distinct peaks using the software WxDiff[34] and sets of experimental scattering amplitudes (F_{obs}) and quasi-unit weights[35] (W_q in Equation 2) were calculated. In order to obtain proper integrated intensity values, peaks were only considered if a proper removal of the intensity background was possible. Peaks for which there was a significant degree of overlap with intensity tails from close neighbor peaks, e.g. the (–21L) rod of TIPS-thiotetracene (Figure 2b left), were therefore not considered. In the case of TIPS-pentacene GIXD images, the removal

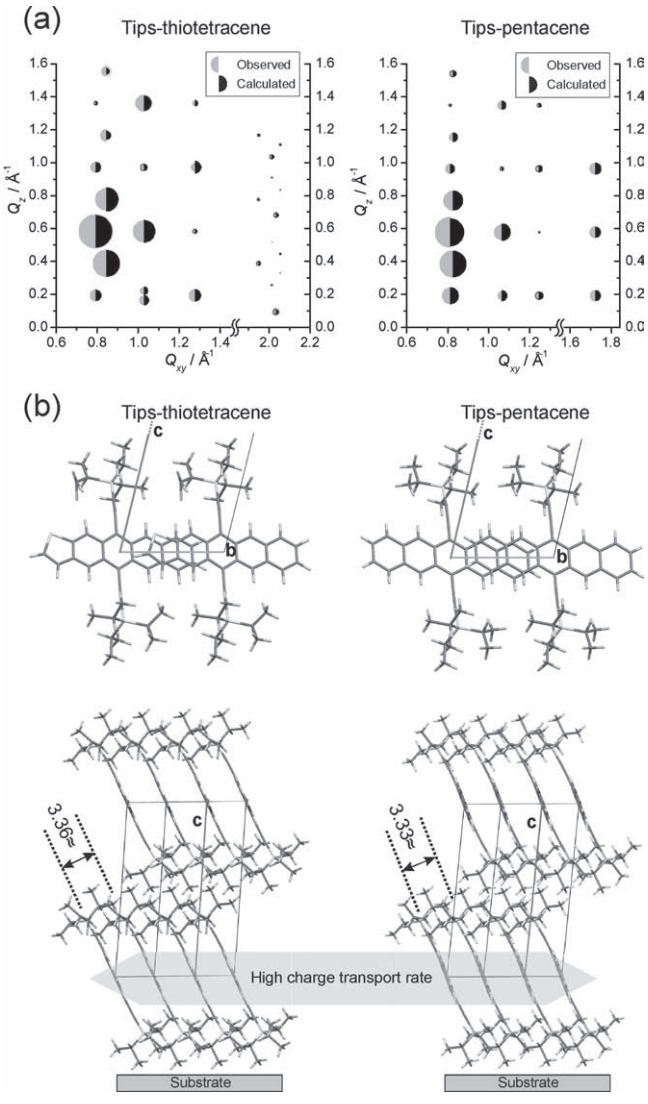

Figure 3. (a) The measured and calculated diffraction intensities (best-fit) for 40nm TIPS-thiotetracene (left) and TIPS-pentacene (right) grown on SiO_2 at 60 °C substrate temperature. The diffraction intensity is indicated by the area of half-circles. (b) The corresponding best-fit molecular packing motifs for TIPS-thiotetracene (left) and TIPS-pentacene (right). Like in the respective single crystal structures, the molecules exhibit a slipped π–π stacking. This stacking direction lies in planes parallel to the substrate plane and forms a highly semiconducting channel for hole transport.

of the background prior to the peak integration was particularly important due to the powder arch segments that intersect some of the peaks (see Figure 2b). The best fit results and corresponding thin film structures of TIPS-thiotetracene and TIPS-pentacene after 2.5 million Monte Carlo steps are shown in **Figure 3** (repetitions of the procedure lead to identical optimal configurations in all cases.)

A very good fit between observed and calculated intensities was obtained for both materials. The corresponding best-fit molecular packing motifs, shown in Figure 3b, are very similar to the respective single crystal structures in which the aromatic cores form slipped π–π stacks. The top part of Figure 3b illustrates this for the molecular dimers as looked down on along the respective a-axes of the unit cell. In the thin films on SiO_2, this slipped-stack direction lies in the substrate surface plane (Figure 3b bottom) which explains the high performance of the respective OTFT devices (the source-drain electrical generates an electrical current that is confined to molecular planes parallel to the substrate). The shortest vertical approach between the aromatic thiotetracene and pentacene sub-units in these motifs was calculated by finding the best-fit set of parallel planes that are populated by the atoms in these molecular cores. The resulting values, 3.36 Å and 3.33 Å, are very similar to the values that had been determined for the corresponding single crystal (3.47 Å and 3.42 Å).

In GIXD experiments on organic thin films, most commonly only the peak positions are measured to determine the unit cell parameters. However, the in the present case excellent agreement between calculated and measured diffraction intensities strongly suggests that it is beneficial to consider both peak positions *and* peak intensities. With the assumption of rigid molecules, the molecular alignment of the bulk structure is virtually replicated by our crystallographic refinement approach, despite the fact that the number of peaks available for intensity analysis from area-detector type GIXD images is about 100 times less than in single crystal X-ray diffraction (refinement is based on many thousands of peaks).

In summary, the thin films of TIPS-thiotetracene and TIPS-pentacene grown on SiO_2 exhibit a molecular packing that is nearly identical to that in the respective bulk crystal structure and there is no indication of polymorphism or thin-film phases as are observed for both aromatic core materials pentacene[15,23] and thiotetracene.[20]

Experimental Section

TIPS-pentacene and TIPS-thiotetracene were purified by three consecutive re-crystallizations in degassed hexanes. Purification by sublimation resulted mainly in decomposition and a very low yield. Thin films of a nominal thickness of 40 nm were vacuum-deposited onto clean SiO_2 substrates (piranha solution and UV/Ozone plasma-treated) at a substrate temperature of 60° and a deposition rate around 0.3 Å/s. These are typical deposition parameters used to produce high-performance OTFTs. GIXD measurements were carried out at the Stanford Synchrotron Radiation Laboratory (SSRL) on beam line 11–3 with a photon energy of 12.73 keV. The incidence angle α of the incident beam was set to 0.1°. The diffraction intensity was detected on a 2D image plate (MAR-345). The distance L = 402 mm between sample and detector was calibrated using a LaB_6 polycrystalline standard. The flat image plate detector records an image of the q-space with distorted geometry and the necessary image correction procedure, enabling direct measurement in the images, is described in more detail in ref. [15]. Numerical integration of the diffraction peak areas and the crystallographic refinement were both performed with the software WxDiff.[34] Before the peak integration, the background was subtracted using a non-parametric algorithm that is similar to Loess, but employs a Gaussian weighting function. The Monte-Carlo optimization of the crystallographic residual was performed with an in-house developed software, POWERGRID.[36]

Supporting Information

Supporting Information is available from the Wiley Online Library or from the author.

Received: August 30, 2010
Published online: November 22, 2010

[1] J. E. Anthony, D. L. Eaton, S. R. Parkin, *Org. Lett* **2002**, *4*, 15.
[2] S. K. Park, T. N. Jackson, J. E. Anthony, D. A. Mourey, *Appl. Phys. Lett.* **2007**, *91*, 063514.
[3] M. M. Payne, S. R. Parkin, J. E. Anthony, C. Kuo, T. N. Jackson, *J. Am. Chem. Soc.* **2005**, *127*, 4986.
[4] M. L. Tang, A. D. Reichardt, T. Siegrist, S. C. B. Mannsfeld, Z. Bao, *Chem. Mater* **2008**, *20*, 4669.
[5] J. E. Anthony, J. S. Brooks, D. L. Eaton, S. R. Parkin, *J. Am. Chem. Soc* **2001**, *123*, 9482.
[6] Z. Bao, J. J. Locklin, *Organic Field-Effect Transistors*; CRC, **2007**.
[7] J. J. Locklin, M. Roberts, S. Mannsfeld, Z. Bao, *J. Macromol. Sci. Polymer Rev.* **2006**, *46*, 79.
[8] S. Liu, W. M. Wang, BA. L. Briseno, S. C. B. Mannsfeld, Z. Bao, *Adv. Mater.* **2009**, *21*, 1217.
[9] M. L. Chabinyc, A. Salleo, *Chem. Mater.* **2004**, *16*, 4509.
[10] J. Rivnay, L. H. Jimison, J. E. Northrup, M. F. Toney, R. Noriega, S. Lu, T. J. Marks, Facchetti, A. Salleo, *Nat. Mater.* **2009**, *8*, 952.
[11] A. Amassian, V. A. Pozdin, T. V. Desai, S. Hong, A. R. Woll, J. D. Ferguson, J. D. Brock, G. G. Mallliaras, J. R. Engstrom, *J. Mater. Chem.* **2009**, *19*, 5580.
[12] A. Amassian, T. V. Desai, S. Kowarik, S. Hong, A. R. Woll, G. G. Mallliaras, F. Schreiber, J. R. Engstrom, *J. Chem. Phys.* **2009**, *130*, 124701.
[13] V. Coropceanu, J. Cornil, D. A. da Silva Filho, Y. Olivier, R. Silbey, J. Brédas, *Chem. Rev.* **2007**, *107*, 926.
[14] C. Reese, Z. Bao, *Adv. Mater.* **2007**, *19*, 4535.
[15] S. C. B. Mannsfeld, A. Virkar, C. Reese, M. F. Toney, Z. Bao, *Adv. Mater.* **2009**, *21*, 2294.
[16] S. C. B. Mannsfeld, J. Locklin, C. Reese, M. E. Roberts, A. J. Lovinger, Z. Bao, *Adv. Func. Mater.* **2007**, *17*, 1617.
[17] X. Feng, V. Marcon, W. Pisula, M. R. Hansen, J. Kirkpatrick, F. Grozema, D. Andrienko, K. Kremer, K. Müllen, *Nat. Mater.* **2009**, *8*, 421.
[18] J. E. Anthony, *Chem. Rev.* **2006**, *106*, 5028.
[19] H. Moon, R. Zeis, E. J. Borkent, C. Besnard, A. J. Lovinger, T. Siegrist, C. Kloc, Z. Bao, *J. Am. Chem. Soc.* **2004**, *126*, 15322.
[20] Q. Yuan, S. C. B. Mannsfeld, M. L. Tang, M. F. Toney, J. Lüning, Z. Bao, *J. Am. Chem. Soc* **2008**, *130*, 3502.
[21] R. Ruiz, A. C. Mayer, G. G. Malliaras, B. Nickel, G. Scoles, A. Kazimirov, H. Kim, R. L. Headrick, Z. Islam, *Appl. Phys. Lett.* **2004**, *85*, 4926.
[22] A. C. Mayer, A. Kazimirov, G. G. Malliaras, *Phys. Rev. Lett.* **2006**, *97*, 105503.
[23] I. P. M. Bouchoms, W. A. Schoonveld, J. Vrijmoeth, T. M. Klapwijk, *Synth. Met.***1999**, *104*, 175.

[24] Q. Yuan, S. C. B. Mannsfeld, M. L. Tang, M. Roberts, M. F. Toney, D. M. DeLongchamp, Z. Bao, *Chem. Mater.* **2008**, *20*, 2763.
[25] T. N. Krauss, E. Barrena, X. N. Zhang, D. G. deOteyza, J. Major, V. Dehm, F. Würthner, L. P. Cavalcanti, H. Dosch, *Langmuir* **2008**, *24*, 12742.
[26] J. Chen, J. Anthony, D. C. Martin, *J. Phys. Chem. B* **2006**, *110*, 16397.
[27] D. T. Cromer, J. B. Mann, *Acta Crystallogr., Sect. A* **1968**, *24*, 321.
[28] R. F. Stewart, E. R. Davidson, W. T. Simpson, *J. Chem. Phys.* **1965**, *42*, 3175.
[29] B. L. Henke, E. M. Gullikson, J. C. Davis, *At. Data Nucl. Data Tables* **1993**, *54*, 181.
[30] D. W. M. Hofmann, T. Lengauer, *J. Mol. Struct.* **1999**, *474*, 13.
[31] G. M. Day, S. L. Price, M. Leslie, *Cryst. Growth Des.* **2001**, *1*, 13.
[32] A. Brunger, *Acta Crystallogr., Sect. A* **1989**, *45*, 42.
[33] S. Kirkpatrick, C. D. Gelatt Jr, M. P. Vecchi, *Science* **1983**, *220*, 671.
[34] S. C. Mannsfeld, *WxDiff*; Stanford Synchrotron Radiation Lightsource, **2009**.
[35] D. Watkin, *J. Appl. Crystallogr.* **2008**, *41*, 491.
[36] S. C. B. Mannsfeld, T. Fritz, *Phys. Rev. B* **2005**, *71*, 235405.